

SPARC/SFN Interaction, Suppresses Type I Collagen in Dermal Fibroblasts

Claudia Chavez-Muñoz,¹ Ryan Hartwell,¹ Reza B. Jalili,¹ Seyed Mehdi Jafarnejad,² Amy Lai,¹ Layla Nabai,¹ Abdi Ghaffari,¹ Peymon Hojabrpour,³ Natalia Kanaan,⁴ Vincent Duronio,³ Emma Guns,⁵ Artem Cherkasov,⁴ and Aziz Ghahary^{1*}

¹Department of Surgery/Plastic Surgery, UBC, Vancouver British Columbia, Canada

²Department of Dermatology, UBC, Vancouver British Columbia, Canada

³Department of Medicine, UBC, Vancouver British Columbia, Canada

⁴Department of Medicine Division of Infectious Diseases, UBC, Vancouver British Columbia, Canada

⁵Department of Urological Sciences, UBC, Vancouver British Columbia, Canada

ABSTRACT

We previously suggested that keratinocyte releasable factors might modulate the wound healing process by regulating the expression of key extracellular matrix components such as collagenase (matrix metalloproteinase-1) and type I collagen in fibroblasts. The first one, we called it keratinocyte-derived anti-fibrogenic factor (KDAF), identified as stratifin (SFN) also named 14-3-3 σ , revealing a strong collagenase activity. However, the second factor, which we named keratinocyte-derived collagen-inhibiting factor(s) (KD-CIF) that has shown to control the synthesis of type I collagen, was not known. Upon conducting a series of systematic protein purification methods followed by mass spectroscopy, two proteins: secreted protein acidic rich in cystein (SPARC) and SFN were identified in keratinocyte-conditioned media. Using co-immunoprecipitation and 3D modeling, we determined that SFN and SPARC form a complex thereby controlling the type I collagen synthesis and expression in fibroblasts. The levels of these proteins in fibrotic tissues (animal and human) were also evaluated and a differential expression of these proteins between normal and fibrotic tissue confirmed their potential role in development of fibrotic condition. In conclusion, this study describes for the first time an interaction between SPARC and SFN that may have implications for the regulation of matrix deposition and prevention of dermal fibrotic conditions such as hypertrophic scars and keloid. *J. Cell. Biochem.* 113: 2622–2632, 2012. © 2012 Wiley Periodicals, Inc.

KEY WORDS: EXTRACELLULAR MATRIX; HYPERTROPHIC SCARS; KERATINOCYTE-DERIVED COLLAGEN INHIBITING FACTOR; STRATIFIN; SPARC

Hypertrophic scars (HS) are characterized by large amounts of extracellular matrix (ECM) deposition, altered in composition and organization compared to that of normal skin [Ladak and Tredget, 2009]. Delayed epithelialization during the process of wound healing also increases the frequency of development of HS [Deitch et al., 1983]. These observations suggest that signals derived from epithelial cells regulate the maturation and remodeling of the wound healing process [Machesney et al., 1998].

Type I collagen (COL1A1) is the most abundant and fibrous form of all collagens produced by fibroblasts [Cutroneo, 2003]. Excessive deposition of COL1A1 results in excessive scarring and HS. An increasing body of evidence suggests that keratinocytes are able to regulate the expression of COL1A1 in dermal fibroblasts [Wood and Stoner, 1996; Ghahary et al., 2004; Harrison et al., 2006]. This regulation is primarily mediated by releasable factors acting in an autocrine/paracrine loop and to a lesser extent direct cell-to-cell

Abbreviations used: ECM, extracellular matrix; FPLC, fast protein liquid chromatography; HS, hypertrophic scar; KCM, keratinocyte-conditioned media; KD-CIF, keratinocyte-derived collagen-inhibiting factor(s); MMP-1, matrix metalloproteinase-1; SFN, stratifin; SPARC, secreted protein acidic rich in cystein.

Conflict of interests: The authors state no conflict of interest.

Additional supporting information may be found in the online version of this article.

Grant sponsor: Canadian Institute of Health Research (CIHR).

*Correspondence to: Dr. Aziz Ghahary, 550-2660 Oak St., Vancouver BC, V6H3Z6 Canada.

E-mail: aghahary@mail.ubc.ca

Manuscript Received: 13 February 2012; Manuscript Accepted: 8 March 2012

Accepted manuscript online in Wiley Online Library (wileyonlinelibrary.com): 15 March 2012

DOI 10.1002/jcb.24137 • © 2012 Wiley Periodicals, Inc.

contact [Ralston et al., 1997; Nowinski et al., 2004; Harrison et al., 2005; Ghaffari et al., 2006].

Our group has previously identified stratifin (SFN) as a potent stimulator of matrix metalloproteinase-1 (MMP-1) expression in dermal fibroblasts [Ghahary et al., 2004]. We have also reported a significant decrease in the expression of COL1A1 in human fibroblasts that have been either co-cultured with keratinocytes or treated with keratinocyte-conditioned media (KCM) (at the mRNA and protein level) [Ghahary et al., 2004; Ghaffari et al., 2009]. Previous characterization of this keratinocyte-derived collagen-inhibitory factor (KD-CIF) revealed a >30 kDa MW protein, which has shown stability up to 56°C and in an acidic environment of pH 2.0 [Ghaffari et al., 2009]. In this study, we identified two proteins that are released by keratinocytes, which interact demonstrating a significant collagen-inhibiting effect in dermal fibroblasts. We also evaluated the physiological levels of these two proteins in a fibrotic animal model and human HS tissues. In conclusion, these findings demonstrate that COL1A1 expression in fibroblasts is modulated by a novel keratinocyte-derived secreted protein acidic rich in cysteine (SPARC)/SFN interaction.

MATERIALS AND METHODS

CELL CULTURE

Following informed consent, foreskins were obtained from neonates undergoing circumcision. Foreskins were washed with PBS 1% antibiotic-antimycotic preparation (100 U/ml penicillin, 100 µg/ml streptomycin, and 0.25 µg/ml amphotericin B) (GIBCO, Carlsbad, CA) and epidermal and dermal layers were separated using dispase (Roche, Laval, QC). Keratinocytes and fibroblasts were cultured as previously described [Ghahary et al., 2000].

CO-CULTURE SYSTEM

The co-culture model was previously described [Ghaffari et al., 2006]. To assemble the co-culture system, inserts containing either keratinocytes or fibroblasts (0.25×10^6) (upper chamber) were placed on top of the fibroblasts (0.5×10^6) (bottom chamber) seeded in six-well plates and cultured with test medium [Ghaffari et al., 2006]. Fibroblasts were harvested at either 24 h for RNA extraction or 48 h for protein extraction, and analyzed using q-PCR or Western blot analysis.

PROTEIN PURIFICATION

Ninety to ninety-five percent confluent keratinocytes were switched to grow in 49.5% KSMF no supplements, plus 49.5% DMEM, plus 1% antibiotic-antimycotic. KCM was collected every 24 h for a period of 10 days, were centrifuged to remove any cell debris and concentrated. Five hundred milligrams of protein was subjected to fast protein liquid chromatography (FPLC) system ÄKTAFFPLC™ (General Electric, Piscataway, NJ). First an anion-exchange column MonoQ™ (General Electric) was used and then a size-exclusion column Superdex™ 75 HR gel filtration column (General Electric). To calibrate the size-exclusion column, Aldolase (158 kDa), Albumin (66.4 kDa), Ovalbumin (43 kDa) and Ribonuclease A (13.7 kDa) were used as standards. The fractions from the anion-

exchange column were desalted using Zeba desalting spin columns (Pierce, Rockford, IL). Fibroblasts were treated with desalted fractions complemented with test medium. Only active fractions were subjected to the size exclusion column. After fractions were collected, fibroblasts treatment steps were repeated. The active fractions were subsequently examined by electrophoresis on a gradient 4–20% Mini-PROTEAN® TGX™ Precast Gel (BioRad, Mississauga, ON) and stained with SYPRO Ruby (Invitrogen, Carlsbad, CA). Bands were cut and analyzed by proteomics.

PROTEOMICS

Active fraction (in solution) and their bands were trypsin digested. The resulting peptides were separated using a 75 µm × 100 mm × 1.7 µm BEH130 C18 column using a 3–40% linear acetonitrile gradient, with 0.1% FA present, at 0.3 µl/min over 40 min using a NanoAcquity™ LC (Waters, Milford, MA). Column elute was directed into a Synapt™ mass spectrometer through a 20 µm capillary held at 3.2 kV. The instrument was run in V-mode with a mass resolution of approximately 10,000. A data dependent method was used with a 1 s scan followed by up to three fragment scans, using ion intensity and charge state as the main selection criteria. The accumulated data was analyzed using ProteinLynx Global Server software using peptide and fragment mass accuracies of 25 ppm and 0.1 Da, respectively. Uniform carbamidomethyl C and variable N-terminal acetyl, M oxidation, N deamidation and C propionamide were selected as permitted modifications with a maximum protein MW of 250 K. This search engine was applied to the full Uniprot database, human species. A search with similar parameters was also carried out using Mascot using the .pkl peak list files generated in PLGS.

PROBABILITY-BASED MOWSE SCORE

Ions score is $-10 \times \log(P)$, where P is the probability that the observed match is a random event. Individual ions scores >40 indicate identity or extensive homology ($P < 0.05$). Protein scores are derived from ions scores as a non-probabilistic basis for ranking protein hits.

WESTERN BLOT ANALYSIS

After 48 h, cell samples were lysed and prepared as previously described [Chavez-Munoz et al., 2009]. Ten to twenty micrograms were loaded into SDS-PAGE. Thirty microliters of KCM samples were loaded into polyacrylamide gels. Western blot was performed as previously described [Chavez-Munoz et al., 2009]. An anti- α 1(I) mAb (1:100) (University of Iowa, Iowa city, IA), or anti-SPARC mAb (1:10,000) (Hematologic Technologies Inc., Essex, VT), or anti-SFN mAb (1:1,000) (NeoMarkers, Fremont, CA), or anti-SFN polyAb (1:1,000 dilution) provided by Dr. Aitken (University of Edinburgh, Scotland), were used as primary antibodies. An anti- β actin mAb (1:30,000) (SIGMA, Saint Louis, MO) was used as loading control. Further, membranes were incubated with goat anti-mouse (800 nm wavelength) or anti-rabbit (680 nm wavelength) IgG IRDye secondary antibody (LI-COR, Lincoln, NE) and analyzed using an Odyssey system (LI-COR).

MODELING METHODS

The ClusPro [Comeau et al., 2004ab; Kozakov et al., 2006, 2010] web-based server was used in order to obtain the protein-protein docking model, where the PDB X-ray structures of 1SRA [Hohenester et al., 1996] (SPARC) and 1YZ5 [Benzinger et al., 2005] (SFN) were used as ligand-receptor, respectively. The most populated and balanced structure was chosen as the best protein-protein interaction model. Then, by means of the molecular operating environment (MOE) [Chemical Computing Group, 2009], the residues of the ligand (receptor) closer than 2.5, 3.5, or 5.0 Å of the receptor (ligand) were computed.

CO-IMMUNOPRECIPITATION (CO-IP)

Co-IP was performed as previously described [Garate et al., 2007]. Briefly, 500 µg of total proteins from KCM was incubated with protein G-sepharose beads and 1 µg of rabbit anti-SFN mAb (NeoMarkers). Immunoprecipitates (IPs) samples were washed three times with PBST, resuspended in 40 µl of sample buffer and run on a SDS-PAGE. Membranes were probed for anti-SFN polyAb (University of Edinburgh, Scotland), and anti-SPARC m-Ab (Hematologic Technologies Inc.) at dilutions mentioned above. The remaining supernatants from IP were kept frozen for further functional assay.

For the functional assay, fibroblasts were treated with 200 µl of the remaining IgG and IP supernatants. After 48 h, fibroblasts were harvested, lysed and analyzed for pro- α 1(I) collagen expression using Western blot.

VALIDATION OF TYPE I COLLAGEN-INHIBITING EFFECT OF hSPARC/RHSFN COMPLEX

Fibroblasts cultured in DMEM 2% FBS were treated with either various concentrations of hSPARC (Hematologic Technologies Inc.) (0.5, 1, 1.5, 2, 5, 10 µg/ml) or with various concentrations of rhSFN (0.5, 1, 1.5, 2, 5, 10 µg/ml) separately, and analyzed for COL1A1 expression at mRNA and pro- α 1(I) collagen at the protein levels. Untreated fibroblasts (C), or treated with 49% KCM were used as negative and positive controls, respectively.

To demonstrate whether hSPARC/rhSFN complex functions as a collagen-inhibitory factor in fibroblasts, fibroblasts cultured in DMEM 2% FBS were treated with constant amount of hSPARC (1.5 µg) plus various concentrations of rhSFN (0.5, 1, 1.5, 2, 5, 10 µg/ml). After either 24 h or 48 h fibroblasts were harvested for either mRNA or protein. Untreated fibroblasts (C) were used as negative control. Fibroblasts treated with 49% of KCM (KCM) or 1.5 µg/ml of hSPARC (SPARC) or 5 µg of hSFN (SFN) served as positive controls.

QUANTITATIVE-PCR (Q-PCR)

Following 24 h of treatment, total RNA was extracted from cell samples. RNA sample was reverse transcribed using the Superscript[®] first-strand synthesis system (Invitrogen). For amplification process, the following sense and anti-sense primers shown in Table S1 were used on an AB 7900HT PCR System (Applied Biosystems, Foster City, CA). Target gene expression was normalized to β -actin levels, and the comparative cycle threshold (C_t) method was used to calculate relative quantification of target mRNAs. Each assay was performed in triplicate with an *n* of 3–5 independent experiments.

TISSUE SAMPLES

To evaluate fibrotic scar formation in vivo, we utilized a well-established rabbit ear model [Morris et al., 1997]. Four female adult New Zealand white rabbits (2.5–3 kg) were used in this study. Four, 8 mm in diameter excisional wounds were created on the ventral surface of each ear using a punch biopsy device. The punch involved the removal of a circular, full-thickness tissue sample down to but not including the cartilage. After 28 days, animals were sacrificed and wounds were harvested (HS). Normal skin from each ear was used as controls (C). Thirty micrograms of tissue was used for mRNA extraction using Mini RNeasy Fibrous Tissue Kit (Qiagen, Mississauga, ON).

For human samples, punch biopsies were collected following informed consent from patients undergoing HS excision. Tissues were fixed in 10% formalin and paraffin embedded.

IMMUNOHISTOCHEMISTRY

Tissue samples were fixed with 10% formalin prior to paraffin embedding. Sections (4 µm) were then prepared and mounted on slides for staining. Antigen retrieval was performed using Citrate Buffer (pH 6.0), microwaved at high power for 17 min. Immunohistochemical staining of SPARC and SFN was achieved using previously mentioned antibodies. Biotinylated goat anti-mouse secondary (Vector Laboratories, Burlingame, CA) was used followed by signal detection using Vector VIP substrate kit (Vector Laboratories). Counterstaining of nucleus was achieved using methylene green (Vector Laboratories). Images were captured using a Nikon DSR1 camera on a Nikon Eclipse 80i upright microscope and processed using Nikon NIS Elements software.

STATISTICAL ANALYSIS

Data were expressed as mean \pm SD and analyzed using appropriate non-parametric tests (i.e., Kruskal–Wallis) using GraphPad Instat Software (GraphPad, San Diego, CA). A *P*-value of <0.05 was considered statistically significant.

RESULTS

KCM SUPPRESSES COL1A1 EXPRESSION IN FIBROBLASTS

COL1A1 expression in fibroblasts was determined following co-culture with keratinocytes or treated with KCM as previously described [Ghahary et al., 2004]. As shown in Figure 1a, pro- α 1(I) protein expression was 78.1% decreased in fibroblasts co-cultured with keratinocytes (lane K/F*) and 87.1% decreased in fibroblasts when treated with KCM (lane KCM), compared to that of control (lane F) (0.219 ± 0.04 vs. 1; *n* = 4; *P* < 0.01 and 0.129 ± 0.012 vs. 1; *n* = 4; *P* < 0.01, respectively). COL1A1 mRNA expression was also decreased 43.5% in fibroblasts co-cultured with keratinocytes (lane K/F*) and decreased 36.7% in fibroblasts treated with KCM (lane KCM) relative to that of fibroblasts control (lane F) (0.565 ± 0.063 vs. 1; *n* = 4; *P* < 0.05 and 0.633 ± 0.054 vs. 1; *n* = 4; *P* < 0.05, respectively).

To evaluate if keratinocyte-differentiation influenced the pro- α 1(I) expression in fibroblasts, KCM was collected everyday from day 1–6 and used individually to treat fibroblasts. Fibroblasts treated

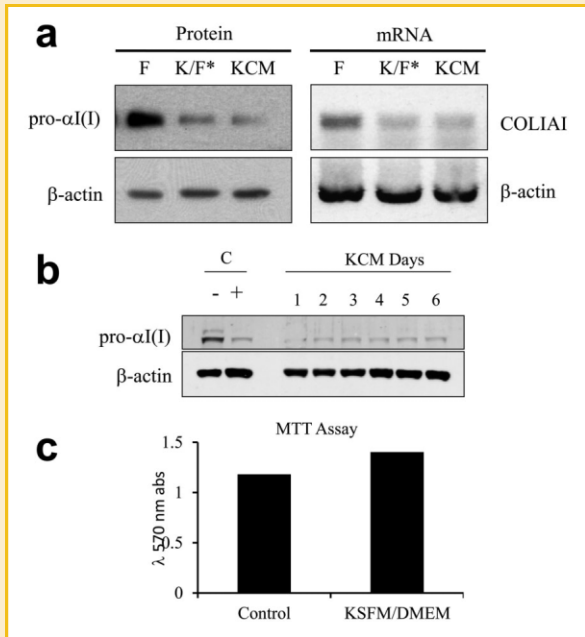


Fig. 1. Keratinocytes regulate type I collagen in fibroblasts. **a:** Protein and mRNA was extracted from fibroblasts co-cultured with keratinocytes (*K/F*), and fibroblasts treated with KCM (*KCM*) as well as fibroblasts untreated (*F*) and subjected to Western blot analysis and q-PCR. All samples were tested for type I collagen and β -actin as loading control. The results showed that pro- α 1(I) and COL1A1 expression was decreased in fibroblasts co-cultured with keratinocytes (78.1% and 43.5%, respectively) (0.219 ± 0.04 vs. 1; $n = 4$; $**P < 0.01$ and 0.565 ± 0.063 ; $n = 4$; $*P < 0.05$, respectively) (*K/F*) and decreased when treated with KCM (87.1% and 36.7%, respectively) (0.129 ± 0.012 vs. 1; $n = 4$; $**P < 0.01$ and 0.633 ± 0.054 ; $n = 4$; $*P < 0.05$, respectively) (*KCM*) compared to that of control (*F*). **b:** Fibroblasts were treated in triplicates with different KCM collection days (D1–D6). Fibroblasts treated with KCM D1–D6 pool (*C+*) and untreated (*C-*) were used as positive and negative control respectively. Samples were subjected to Western blot analysis and proved for pro- α 1(I) collagen. β -actin was used as a loading control. The results showed that pro- α 1(I) was decreased in fibroblasts treated with KCM from day 1–6 (lanes 1–6 KCM days) as well as when treated with the pooled KCM (*C+*) when compared to that of untreated fibroblasts (*C-*). (Image representative of an $n = 3$). **c:** Keratinocytes in culture with KSFM/DMEM media without supplements (*K/D*) as well as keratinocytes cultured in KSFM+suppl. media (*Control*) through out 10 days were subjected to MTT assay to evaluate viability of the cells.

with a pooled sample of KCM from days 1–6 and untreated fibroblasts were used as positive and negative controls, respectively. Figure 1b demonstrated that pro- α 1(I) protein is decreased in fibroblasts treated with KCM from all day (lanes 1–6 KCM days) as well as when treated with the pooled KCM (lane *C+*) when compared to that of untreated fibroblasts (lane *C-*). We have previously demonstrated that involucrin (keratinocyte-differentiation marker), is expressed in KCM since day 4 when cultured in KSFM/DMEM media [Ghahary et al., 2001].

MTT assay was performed to confirm that keratinocytes were viable when cultured in KSFM/DMEM medium in absence of supplements. No significant changes were shown when compared to that of keratinocytes cultured normally (Fig. 1c), suggesting that KSFM/DMEM media did not affect the viability of keratinocytes.

IDENTIFICATION OF KD-CIF

To identify KD-CIF, KCM was subjected to an anion-exchange column. Twenty-one fractions were collected and fibroblasts were treated with pooled samples comprising three fractions (i.e., 1–3; 4–6, etc.). The results showed that fibroblasts treated with fractions 13–15 exhibited a 33.2% decrease in the expression of COL1A1 when compared to that of control (lane FC) (0.668 ± 0.046 vs. 1 ± 0.016 , respectively; $n = 3$; $P < 0.05$) as well as the rest of the treated samples (Fig. 2a). These results were further confirmed at the protein level (Fig. 2b). Then, fibroblasts were treated with fractions 10–21 individually. The q-PCR results showed that fractions 13 and 14 contained the collagen-inhibiting factor(s) as evident by 70% decrease of COL1A1 when compared to that of control (Fig. 2c). To further identify this factor(s), fractions 13 and 14 were passed through a size-exclusion column. Forty-five fractions were collected and fibroblasts were treated individually with these fractions. The results of q-PCR showed that fraction 20 showed a significant COL1A1 reduction (0.447 ± 0.103 ; $n = 3$, $P < 0.01$) when compared to that of the control (Fig. 2d). These results were subsequently confirmed by Western blotting (Fig. 2e). The linear regression of a MW standard curve showed that a LogMW of 4.7166 for fraction 20 represented approximately 52 kDa (Fig. 2f).

In order to identify the KD-CIF, fractions 16–26 were run on a gradient gel, showing a strong band around the 60 kDa in fractions 19–21, and finally disappearing on fraction 26 (Fig. 3a).

Bands from 19 and 20 as well as the total fractions were sent for mass-spectrometry. The results revealed the presence of two known proteins in the bands as well as in the total fraction: SPARC also known as osteonectin (34 kDa), and SFN also known as 14-3-3 σ (28 kDa) (Fig. 3b). As shown in Figure 3b, mass-spectrometry revealed only peptides that matched for SPARC and SFN proteins showing a high MOWSE score.

EXPRESSION OF SPARC/SFN IN KERATINOCYTES AND FIBROBLASTS

Upon identification of SFN and SPARC by mass-spectrometry, we then evaluated the expression of these proteins were evaluated in: keratinocytes (lane K), fibroblasts (lane F) and when fibroblasts co-cultured with either fibroblasts or keratinocytes (lanes F/F* K/F*, respectively) at the mRNA and protein levels. The result of Figure 3c demonstrated the presence of SPARC at the mRNA and protein levels in keratinocytes and fibroblasts and when co-cultured together. Unlike SPARC, SFN is only present in keratinocytes but not in fibroblasts shown at the mRNA and protein level. β -actin was used as a loading control in both settings.

EVALUATION OF SPARC/SFN AS A COMPLEX IN KCM

Knowing that both proteins were produced and released by keratinocytes, we then evaluated the possibility of the formation of a complex by these two proteins under native conditions in KCM. To achieve this, KCM as well as fraction 20 were run on a native non-denaturing gel. The result of Figure 3d reveals that both proteins co-migrated to the same MW on the gel, as both were detected using mouse anti-SPARC and rabbit anti-SFN antibodies and visualizing them under different wavelengths (800 nm and 680 nm, respectively). This result suggested that SFN and SPARC may bind in KCM.

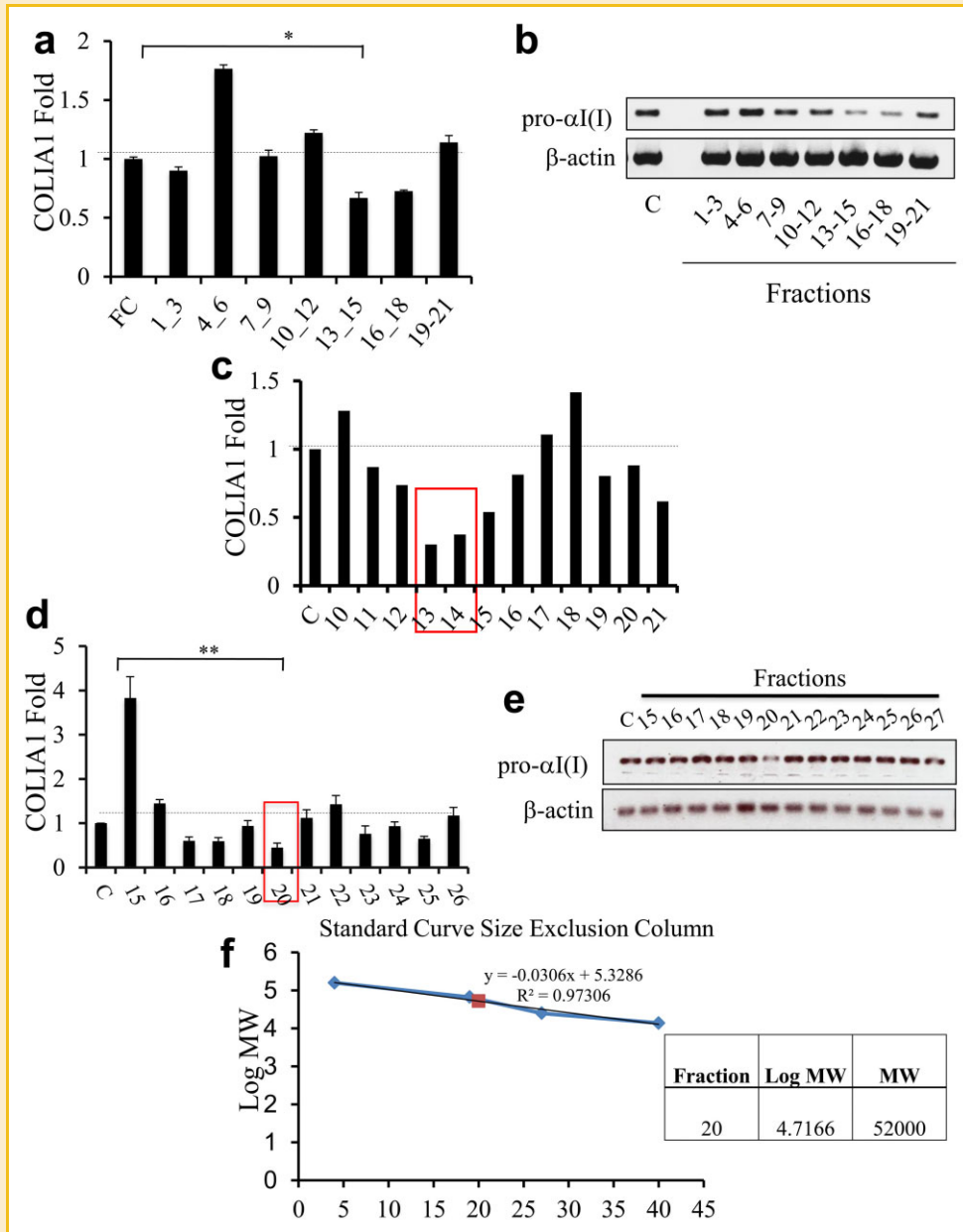


Fig. 2. Purification of KD-CIF. KCM was first passed through an anion-exchange column. Twenty-one fractions were collected. Fibroblasts were treated in triplicates with groups of these fractions and subjected to q-PCR and Western blot analysis. a: Fractions 13–15 presented a 40% decrease in COLIAI mRNA when compared to that of control (FC) (0.668 ± 0.046 vs. 1 ± 0.016 , respectively; $n = 5$; $*P < 0.05$). b: Results were confirmed at the protein level. (Image representative of an $n = 3$). c: Fibroblasts were then treated in triplicates with fractions 10–21 individually. The q-PCR results showed that fractions 13 and 14 contained the collagen-inhibiting factor(s) as evident by 70% decrease of COLIAI when compared to that of control. Only fractions 13 and 14 were passed through a size-exclusion column. d: Fibroblasts were treated in triplicates with the fractions and subjected to q-PCR. The results showed that fraction 20 had the most significant collagen-inhibiting effect (0.447 ± 0.103 ; $n = 3$, $**P < 0.01$) when compared to that of the control. e: Results were confirmed at the protein level. (Image representative of an $n = 3$). f: A standard curve was created using a linear regression. A LogMW of 4.7166 for fraction 20 represented approximately 52 kDa.

To further validate our findings, a Co-IP of KCM was performed by immunoprecipitating SFN and then blotting for SPARC. As shown in Figure 4a, the IP sample showed the presence of SPARC and SFN when precipitated for SFN. These results confirm the interaction between these two proteins in the KCM. To double confirm this finding, we attempted to co-IP SPARC and blot for the presence of SFN. However, we were not able to precipitate SPARC

from KCM as shown in Figure S.6. This finding may suggest that SPARC may be surrounded by SFN molecules encapsulating SPARC and not allowing SPARC antibody to bind to SPARC epitope.

In order to predict how these two proteins could indeed interact in physiological conditions, a 3-D modeling structure was designed (Fig. 4b). The predicted structure showed a populated and balanced structure with rms constraints of 9 Å. Furthermore, possible binding

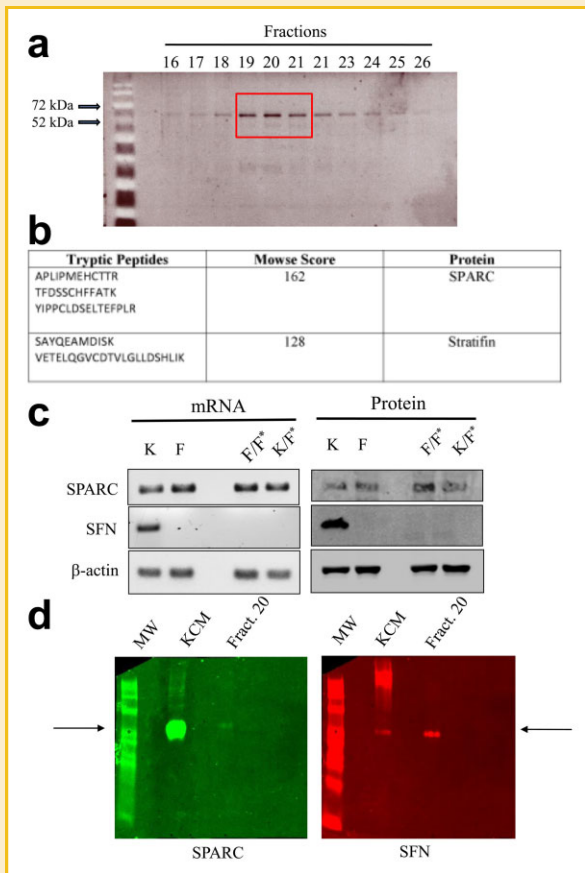


Fig. 3. Identification of KD-CIF. **a:** Fractions 16–26 were run in a gradient gel and stained with SYPRO RUBY. **b:** Bands from 19 and 20 as well as the total fractions were analyzed by mass-spectrometry. The results matched peptide specifically for SPARC and SFN. (*Mowse scores* > 40 indicate identity or extensive homology ($P < 0.05$)). **c:** Keratinocytes (K) and fibroblasts (F) as well as fibroblasts co-cultured with keratinocytes (K/F⁺) and fibroblasts co-cultured with fibroblasts (F/F⁺) were evaluated for the presence of SPARC and SFN at the gene and at the protein level. β -actin was used as a loading control. (*Image representative of an n = 3*). **d:** To evaluate the possibility of these two proteins forming a complex under natural conditions, KCM as well as fraction 20 were run on a native non-denaturing gel. The results show the co-migration of both proteins at a same molecular weight between 52 and 72 kDa.

sites were predicted with rms of 2.5 Å according to the binding characteristics for SFN (Fig. 4c). Two-exposed (surface) Serines (S) and one Threonine (T) were found on SPARC at a close proximity of 3.5 Å to K49 and R56 SFN residues (Fig. 4d). Together these findings suggests the ability of SPARC and SFN to form a complex structure. This 3-D modeling also confirms the impossibility of SPARC antibody to precipitate SPARC protein from KCM.

SPARC/SFN COMPLEX RESPONSIBLE FOR THE COLLAGEN-INHIBITORY EFFECT

To evaluate if the SPARC/SFN complex was in fact responsible for suppressing COL1A1 expression, we treated fibroblasts with the supernatant of IgG and IP samples using untreated and KCM-treated fibroblasts as negative and positive controls, respectively. As shown

in Figure 5a, IgG supernatant revealed a 40% decrease in pro- α 1(I) expression (lane IgG) comparable to that seen when treated with KCM (40% decrease) (lane KCM). This suppression was restored when fibroblasts were treated with the IP supernatant (lane IP) when compared to that of IgG supernatant (lane IgG) (1.348 ± 0.255 vs. 0.807 ± 0.139 ; $n = 4$; $P < 0.01$). This finding demonstrated that when the SPARC/SFN complex is removed from the KCM, pro- α 1(I) levels are as baseline, showing no collagen-inhibitory effect. These results suggest that SPARC/SFN complex may be responsible for type I collagen suppression in fibroblasts.

To further investigate the function of SPARC/SFN as a complex compared to their efficacy independent from one another, fibroblasts were treated with each protein separately. As mentioned under Materials and Methods Section, fibroblasts were treated with different concentrations of rhSFN or hSPARC (0.5, 1, 1.5, 2, 5, and 10 μ g/ml) and type I collagen at the mRNA and protein levels were evaluated. As observed in Figure 5b, when fibroblasts were treated with hrSFN at 0.5 μ g/ml there was a significant reduction in pro- α 1(I) protein expression when compared to that of control (0.70 ± 0.05 vs. 1 ± 0.03 , respectively; $n = 5$; $P < 0.05$), which progressively returned to the baseline levels as the concentration of SFN was increased. A similar trend was observed when fibroblasts were treated with hSPARC, however at a 1.5 μ g/ml concentration, pro- α 1(I) expression was stimulated and progressively increased from baseline in a dose dependent fashion. Similar trend was also found when evaluating COL1A1 mRNA expression (1.48 ± 0.168 vs. 1 ± 0.37 , respectively; $n = 5$; $P < 0.05$) (Fig. 5c).

Importantly, the significant collagen-inhibitory effect of KCM treatment was not observed at any concentration of these proteins when delivered independently.

Fibroblasts were then treated with SPARC and SFN in combination, to evaluate the potential collagen-inhibitory effect (Fig. 5d). Fibroblasts were treated with a fixed dose of 1.5 μ g/ml of hSPARC, and with increasing doses of rhSFN (0.5, 1, 1.5, 2, 5, 10 μ g/ml) (Fig. 5d). Fibroblasts treated with 1.5 μ g/ml of SPARC (lane 1.5 μ g SPARC) and fibroblasts treated with 2 μ g/ml of rhSFN (lane 2 μ g SFN) as well as fibroblasts treated with KCM (lane KCM) or untreated (lane C) were used as controls. The results revealed a significant 70% decrease in COL1A1 expression at both mRNA and protein levels when 1.5 μ g/ml of SPARC plus 1.5 μ g/ml SFN were added to fibroblasts (0.3636 ± 0.066 ; $n = 3$; $P < 0.01$) compared to that of untreated fibroblasts (lane C) or to fibroblasts treated with either 1.5 μ g/ml SPARC or 2 μ g/ml SFN (1.371 ± 0.043 and 1.052 ± 0.006 ; $n = 3$) (Fig. 5d). This effect was maintained while SFN dosage was increased (2, 5 and 10 μ g/ml) and SPARC dosage remained the same (1.5 μ g/ml) (0.93 ± 0.01 ; 0.79 ± 0.02 ; 0.335 ± 0.057 ; $n = 3$; respectively). This finding also supports the earlier computerized docking data, whereby a specific ratio of SPARC/SFN suggests to be required to form the complex and influence collagen expression in dermal fibroblasts.

EVALUATION OF PHYSIOLOGICAL LEVELS OF SPARC AND SFN IN FIBROTIC TISSUES

A fibrotic rabbit ear model was used to evaluate the physiological role of SPARC/SFN. Four, 8-mm diameter wounds were created on rabbits' ears. On day 28 when HSs were formed, tissues were

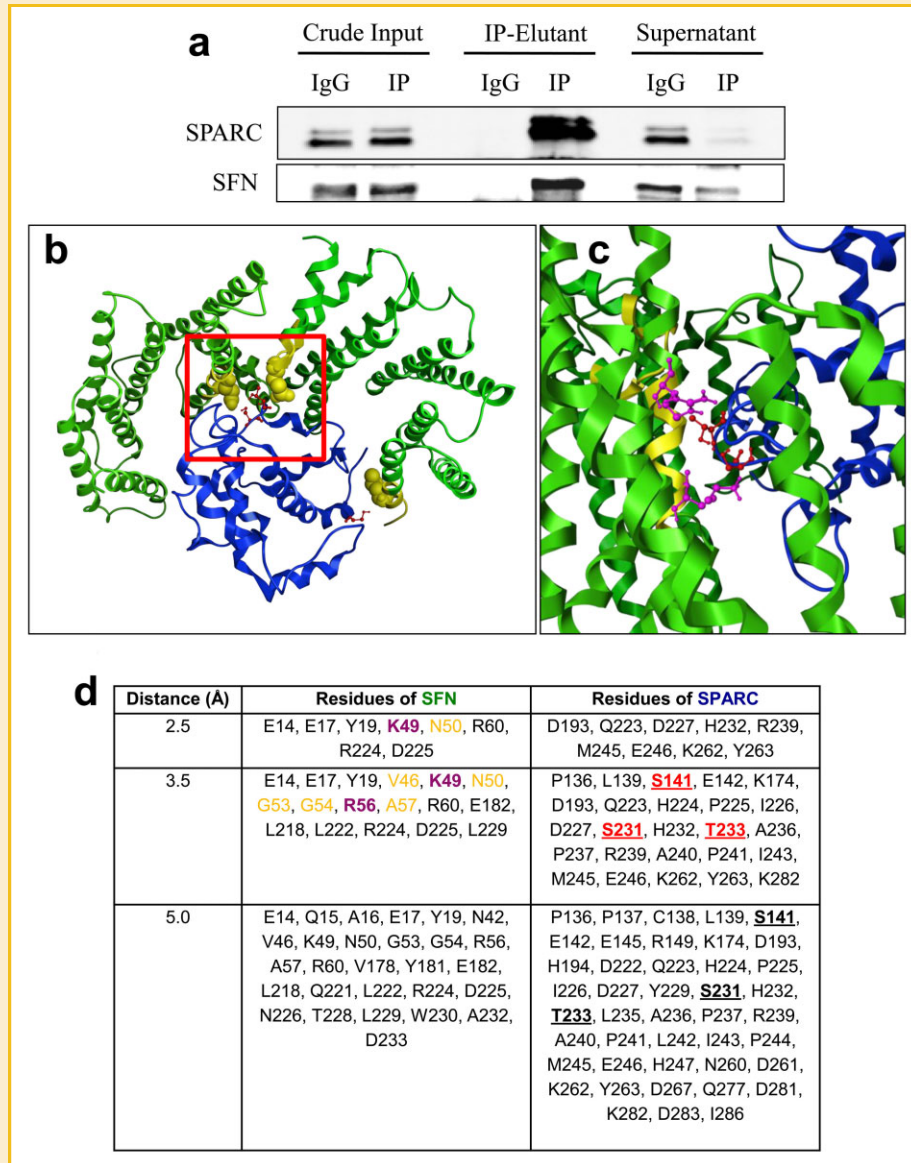


Fig. 4. Evaluation of SPARC/SFN as a complex in KCM. a: Co-immunoprecipitation (Co-IP) on KCM was performed. SFN was precipitated using mouse anti-SFN antibody, IgG and IP from input, IP and supernatant samples were run on a SDS-PAGE and blotted for anti-SPARC antibody. The results showed the presence of SPARC and SFN when immunoprecipitated for SFN. (Image representative of an $n = 4$). In order to predict if these two proteins could indeed form naturally a complex, a 3-D modeling using X-ray structures was designed. b: Protein-protein interaction model. SFN protein is depicted in green and SPARC protein is depicted in blue. The Serine and Threonine residues are highlighted in red and the residues close than 3.5 Å to them are drawn in yellow (the central residues are draft as Van der Waals spheres). c: A closer look at these binding sites between SFN (depicted in green) and SPARC (depicted in blue). Possible phosphorylation sites (S/T) depicted in yellow, and in purple the two well-known residues (K49 and R56), which are part of the SFN "binding groove" at <3.5 Å. d: Residues of the ligand (receptor) closer than 2.5, 3.5, or 5.0 Å of the receptor (ligand). The possible phosphorylated residues of the ligand (SPARC) are depicted in red, and their corresponding binding residues from SFN are depicted in yellow and purple matching panel B image.

harvested and evaluated at mRNA level. The tissue was analyzed using q-PCR for SPARC, SFN and COL1A1 mRNAs. The results show that HS reveal a very significant amount of SPARC when compared to that of control (3.158 ± 0.707 vs. 1; $n = 4$, $P < 0.01$) and very low levels of SFN when compared to that of control (0.342 ± 0.0046 vs. 1; $n = 4$, $P < 0.01$; Fig. 6a). On the other hand, COL1A1 demonstrated a significant increase (14.235 ± 0.535 ; $n = 4$, $P < 0.01$) when compared to that of control.

To further evaluate this pattern, human HS tissues and normal human tissues were also analyzed for SPARC and SFN using

immunohistochemistry. The results demonstrated an increased expression of SPARC and an almost absent expression of SFN in human HS when compared to that of control (Fig. 6b). These results suggest that a balance is probably necessary between SPARC and SFN to maintain type I collagen normal levels.

DISCUSSION

This study provides compelling evidence that keratinocyte-derived factors, such as SPARC/SFN, are essential components of wound

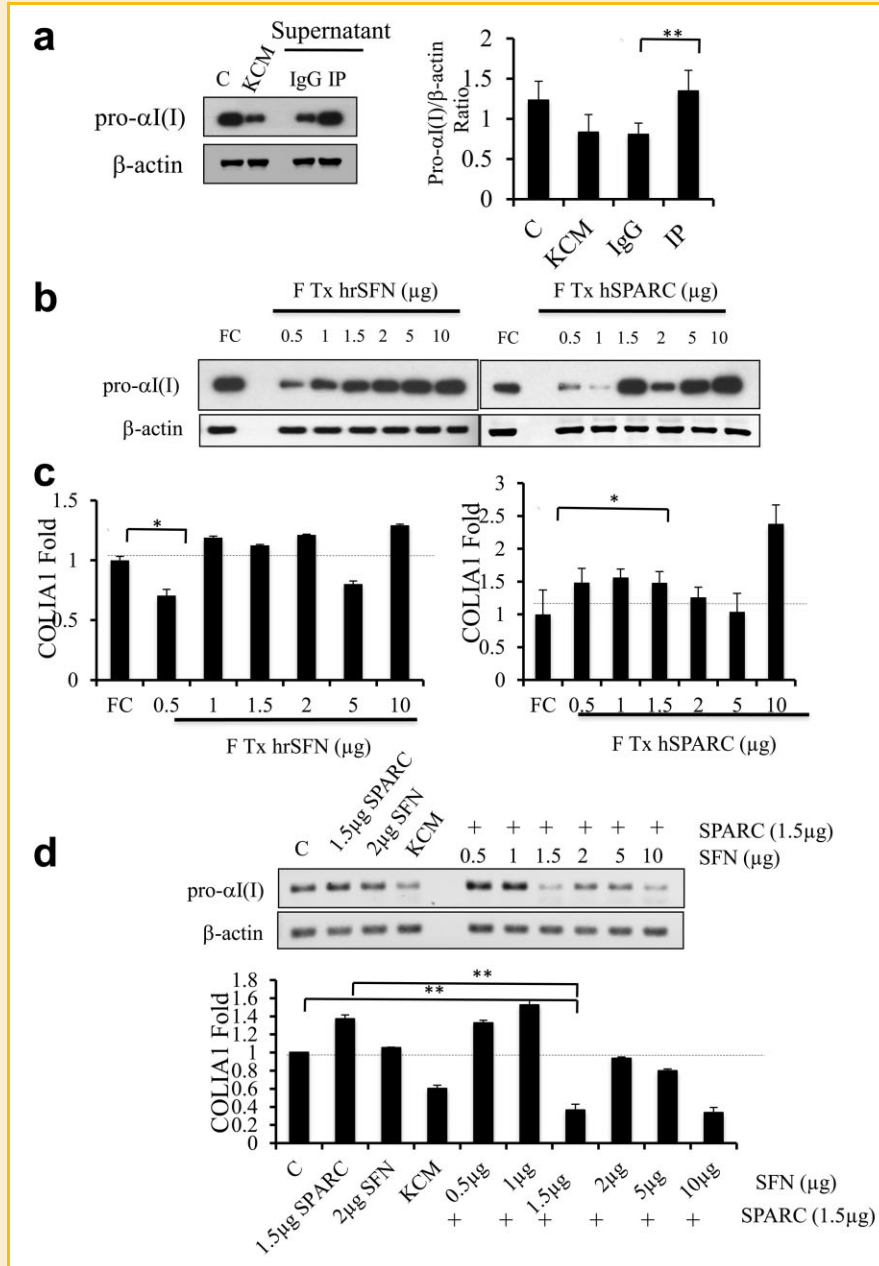


Fig. 5. SPARC/SFN complex responsible for the collagen-inhibitory effect. To evaluate if SPARC/SFN complex was in fact responsible for suppressing collagen expression, (a) fibroblasts were treated with either the supernatant of IgG or IP samples. Untreated or KCM-treated were used as controls. The results showed that when fibroblasts were treated with IgG supernatant it significantly decreased pro-α1(I) expression (40%) (lane IgG) compared to that of when treated with KCM (40% decrease) (lane KCM). This suppression was reverted when fibroblasts were treated with the IP supernatant (lane IP) when compared to that of IgG supernatant (lane IgG) (1.348 ± 0.255 vs. 0.807 ± 0.139 ; $n = 4$; $**P < 0.01$). b: Fibroblasts were treated in triplicate with different concentrations of rhSFN and hSPARC (0.5, 1, 1.5, 2, 5 and 10 μg/ml) and evaluated for pro-α1(I) at the protein and (c) COL1A1 at mRNA levels. Fibroblasts treated with 0.5 μg of rhSFN showed a significant reduction in COL1A1 expression when compared to that of control (0.70 ± 0.05 vs. 1 ± 0.03 , respectively; $n = 5$; $*P < 0.05$), which progressively returned to the baseline levels as the concentration of SFN increased. Similar trend was observed when fibroblasts were treated with hSPARC, however at a 1.5 μg/ml concentration, COL1A1 expression was stimulated and progressively increased from baseline in a dose dependent fashion (1.48 ± 0.168 vs. 1 ± 0.37 , respectively; $n = 5$; $*P < 0.05$). d: To evaluate the collagen-inhibitory effect, fibroblasts were treated with the combination of both proteins. Fibroblasts were treated with a fixed dose of 1.5 μg/ml of hSPARC, and with variable increasing doses of rhSFN (0.5, 1, 1.5, 2, 5, 10 μg/ml). Fibroblasts treated with 1.5 μg/ml of SPARC (lane 1.5 μg SPARC) and fibroblasts treated with 2 μg/ml of rhSFN (lane 2 μg SFN) as well as fibroblasts treated with KCM (lane KCM) or untreated (lane C) were used as controls. Samples were evaluated at the protein (top image) and mRNA levels (bottom Graph). Results revealed 70% decrease in COL1A1 expression at both mRNA and protein levels when a combination of 1.5 μg/ml of SPARC plus 1.5 μg/ml SFN were added to fibroblasts (0.3636 ± 0.066 ; $n = 3$; $**P < 0.01$) compared to that of untreated fibroblasts (lane c) or treated with either 1.5 μg/ml SPARC or 2 μg/ml SFN (1.371 ± 0.043 and 1.052 ± 0.006 ; $n = 3$; $**P < 0.01$). This effect was maintained while SFN dosage was increased.

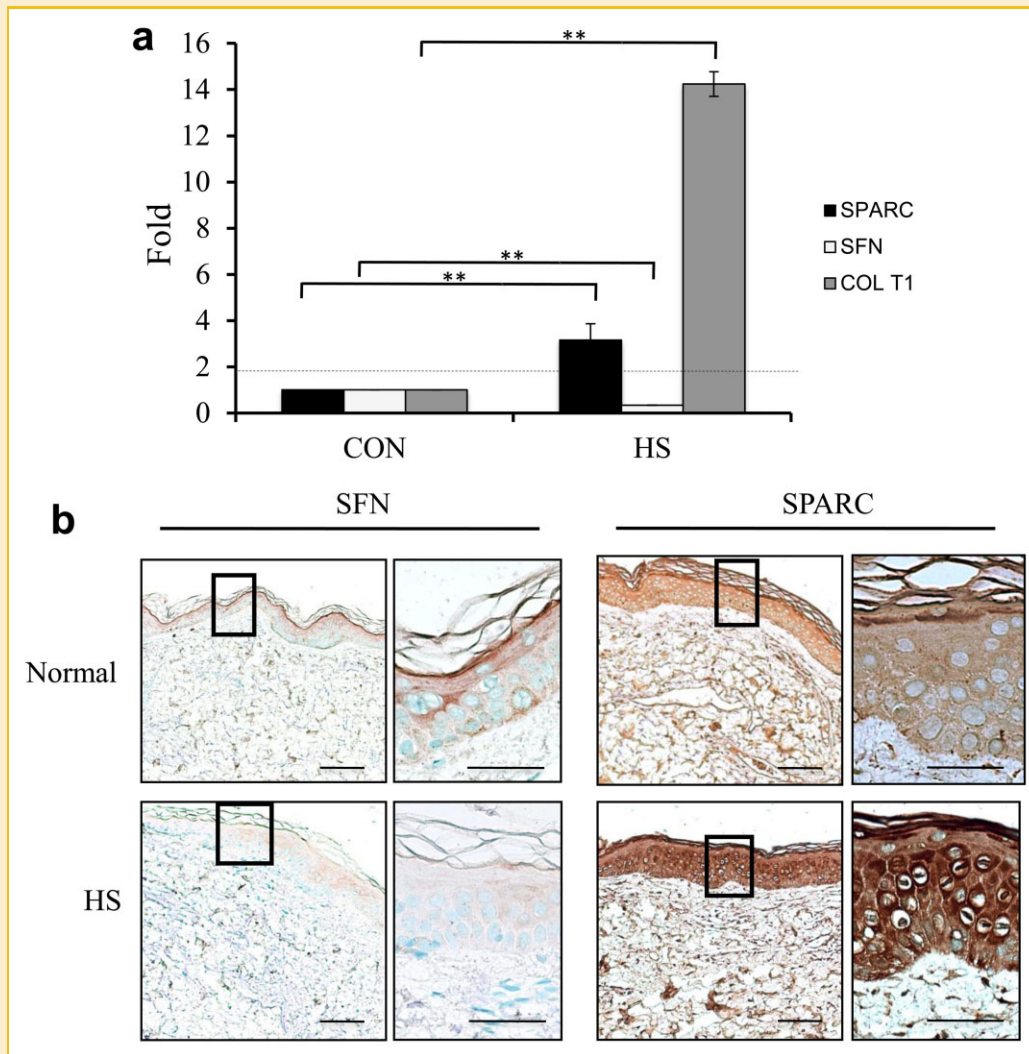


Fig. 6. Physiological levels of SPARC/SFN in fibrotic tissues. a: Rabbit HS tissues were analyzed using q-PCR for SPARC, SFN, and COL1A1. The results show that HS present a very significant amount of SPARC when compared to that of control (3.158 ± 0.707 vs. 1; $n = 4$, $**P < 0.01$) and a very low levels of SFN when compared to that of controls (0.342 ± 0.0046 vs. 1; $n = 4$, $**P < 0.01$). Nonetheless, COL1A1 was highly expressed (14.235 ± 0.535 ; $n = 4$, $**P < 0.01$) when compared to that of control. b: Human HS tissues and normal human tissues were analyzed for SPARC and SFN using immunohistochemistry. The results revealed an increased expression of SPARC and an almost absent expression of SFN in human HS when compared to that of control. Images were taken at low magnification of $10\times$ (planfluor, 0.3NA) with a scale bar of $100\ \mu\text{m}$ and high magnification of $40\times$ (planfluor, 0.75NA) with a scale bar of $50\ \mu\text{m}$. All images were captured using a Nikon DSr1 camera on a Nikon Eclipse 80i upright bright field microscope and processed using Nikon NIS Elements software.

healing physiology that regulate the production and degradation of ECM components. In our previous work, we discovered a keratinocyte-releasable form of SFN that showed a significant MMP-1 stimulatory effect in dermal fibroblasts [Ghahary et al., 2004]. At that time it was also evident that KCM treatment would reduce the gene expression of COL1A1 and that this effect could not be re-created when fibroblasts were treated with recombinant SFN alone [Ghahary et al., 2004]. Toward a deeper explanation of the collagen gene expression suppression by KCM, we have demonstrated in this work that when fibroblasts are co-cultured with keratinocytes or treated with KCM there was a significant reduction in COL1A1 expression at the mRNA and proteins levels (Fig. 1a). Our finding is consistent with previous data from Harrison and Gardner [Gardner, 1998; Harrison et al., 2006], in which they used the N-

terminal pro-peptide of type I collagen in conditioned media of differentiated cells or the incorporation of (^3H) proline as markers for collagen production, revealing also a role for keratinocyte-fibroblast cross talk in regulation of type I collagen.

Keratinocyte differentiation within an in vitro system can result in cell death, and to ensure that the observed collagen was not an artifact of keratinocyte apoptosis in vitro, an MTT assay was performed. The results demonstrated that there was no significant death and therefore a factor or complex of factors that is released from keratinocytes must be responsible for the observed reduction in collagen expression (COL1A1). Next, using mass-spectroscopy we determined that the two most abundant (and only active) proteins in the active FPLC-fraction of KCM were SFN and SPARC.

SFN belongs to the family of 14-3-3 proteins, which are highly conserved molecular chaperons. It was originally thought to be an exclusive intracellular protein due to its lack of signal peptide, but in 1982, Boston et al., [Boston et al., 1982] reported the presence of this protein in cerebrospinal fluid in patients with neurological disorders. Later, Katz and Taichman [1999] found that SFN was secreted into KCM, however no physiological function was assigned to this protein until in 2004 when Ghahary et al. [2004] demonstrated SFN to be a potent MMP-1 stimulatory protein in dermal fibroblasts.

SPARC, also known as osteonectin, or BM-40, is a Ca^{2+} -binding glycoprotein that functions as a counteradhesive protein, modulating cell shape, growth factor activity, and as a cell-cell inhibitor. SPARC is expressed at significant levels in tissues undergoing repair or remodeling due to wound healing process, disease or physiological conditions. Fibroblasts and macrophages start expressing SPARC in healing wounds where it is also released by platelet degranulation [Lane and Sage, 1994]. Pathological conditions such as dermal and lung fibrosis are characterized by elevated expression of SPARC [Reed and Sage, 1996].

We have previously showed that SFN does not inhibit COL1A1 expression in dermal fibroblast [Ghahary et al., 2004]. Conversely, it is known that SPARC is able to stimulate the expression of COL1A1 [Francki et al., 1999]. Collectively, this prior knowledge made the discovery of these two proteins in the active fraction of KCM puzzling, unless there existed an interaction between the two, which resulted in reduced collagen production. In fact, fraction 20 containing SFN (a 28 kDa protein) and SPARC (a 34 kDa protein) corresponded to an approximate molecular weight of 52 kDa.

To confirm this hypothesis, fibroblasts were treated with either rhSFN or hSPARC alone, without observing any collagen-inhibitory effect (Fig. 5b), whereas the concentrated active fraction (containing both proteins) could effectively reduce COL1A1 expression and protein synthesis.

In order to determined whether or not this interaction could physically occur a 3-D structure of the complex was created using known X-ray structures of both SFN and SPARC, revealing a balanced structure with high probability of binding (rms 2.5 Å).

Three protein-protein binding sites were predicted suggesting to occur on phosphorylated Serine (S141, S231) and Threonine (T233) which coincide with the binding characteristics of SFN to other known proteins [Fu et al., 2000; Wilker et al., 2005]. These data further underscore the probability of a naturally occurring SPARC/SFN complex *in vivo*.

Additionally, we demonstrated that when fibroblasts were treated with hSPARC/hrSFN complex, the expression of COL1A1 in fibroblasts was markedly decreased at the mRNA and pro- α 1(I) protein levels. Likewise, when fibroblasts were treated with the supernatant from immunoprecipitation, the collagen-inhibitory effect was removed, suggesting that the complex is indeed responsible for this effect.

Although 14-3-3 proteins are known intracellularly to serve as chaperons [Fu et al., 2000], this is the first indication that SFN (14-3-3 sigma) interacts with SPARC to cause an anti-fibrotic event. In fact, very few extracellular functional roles have been attributed

to either protein. However, the mechanism for the suppression of collagen expression by the SPARC/SFN complex remains to be elucidated, it is reasonable to suggest that SFN might sequester SPARC in the extracellular environment and thus, interfere with ligand and receptor interaction. This interference may result from inhibiting the binding of SPARC to integrins or adaptor proteins and thereby suppressing pro- α 1(I) synthesis. Future investigation focusing on the downstream mechanisms responsible for the SFN/SPARC interaction and reduction in collagen will greatly improve upon the current understanding of the late stage healing process (remodeling).

Notably in the wound environment, differentiated keratinocytes release SFN, whereas numerous skin cells and infiltrated immune cells can release SPARC and thus our findings further support the observation that delay in wound epithelialization can result in fibrotic conditions such as HS [Francki et al., 1999; Rentz et al., 2007; Chlenski and Cohn, 2010]. This was observed when we evaluated the physiological level of SFN, SPARC, and COL1A1 in a fibrotic animal model (Fig. 6a). Similarly, sections from human HS showed a reduction in SFN and an increase in the amount of SPARC (Fig. 6b). Based on our findings, a lack of SFN protein and an overexpression of SPARC cause a greater expression of COL1A1, which may in part, be the reason why these wounds develop HS.

In conclusion, our findings suggest that upon epithelialization, keratinocytes may in fact release SPARC and SFN, which may interact in the extracellular space modulating the expression of ECM components in fibroblasts during the phase of tissue remodeling. The identification of this complex has further provided us with another potential therapeutic agent to treat HS, frequently developed following burn injury, deep trauma, and some surgical incisions.

ACKNOWLEDGMENTS

This study was supported by the Canadian Institute of Health Research (CIHR). Dr. C. Chavez-Munoz holds a CIHR-doctoral graduate award and Michael Smith Foundation for Health Research (MSFHR) Junior award. The authors are grateful to Hans Adomat for his knowledge and expertise in proteomics.

REFERENCES

- Benzinger A, Popowicz GM, Joy JK, Majumdar S, Holak TA, Hermeking H. 2005. The crystal structure of the non-liganded 14-3-3sigma protein: Insights into determinants of isoform specific ligand binding and dimerization. *Cell Res* 15:219-227.
- Boston PF, Jackson P, Thompson RJ. 1982. Human 14-3-3 proteins: Radio-immunoassay, tissue distribution and cerebrospinal fluid levels in patients with neurological disorders. *J Neurochem* 38:1475-1482.
- Chavez-Munoz C, Kilani RT, Ghahary A. 2009. Profile of exosomes related proteins released by differentiated and undifferentiated human keratinocytes. *J Cell Physiol* 221:221-231.
- Chemical Computing Group I Version 2009.10 software. 2009. Molecular Operating Environment (MOE), Montreal, Quebec, Canada.
- Chlenski A, Cohn SL. 2010. Modulation of matrix remodeling by SPARC in neoplastic progression. *Semin Cell Dev Biol* 21:55-65.

- Comeau SR, Gatchell DW, Vajda S, Camacho CJ. 2004a. ClusPro: A fully automated algorithm for protein-protein docking. *Nucleic Acids Res* 32: W96–W99.
- Comeau SR, Gatchell DW, Vajda S, Camacho CJ. 2004b. ClusPro: An automated docking and discrimination method for the prediction of protein complexes. *Bioinformatics* 20:45–50.
- Cutroneo KR. 2003. How is type I procollagen synthesis regulated at the gene level during tissue fibrosis. *J Cell Biochem* 90:1–15.
- Deitch EA, Wheelahan TM, Rose MP, Clothier J, Cotter J. 1983. Hypertrophic burn scars: Analysis of variables. *J Trauma* 23:895–898.
- Francki A, Bradshaw AD, Bassuk JA, Howe CC, Couser WG, Sage EH. 1999. SPARC regulates the expression of collagen T1 and TGF- β 1 in mesangial cells. *J Biol Chem* 274:32145–32152.
- Fu H, Subramanian RR, Masters SC. 2000. 14-3-3 proteins: Structure, function, and regulation. *Annu Rev Pharmacol Toxicol* 40:617–628.
- Garate M, Campos EI, Bush JA, Xiao H, Li G. 2007. Phosphorylation of the tumor suppressor p33ING1b at Ser-126 influences its protein stability and proliferation of melanoma cells. *FASEB J* 21:3705–3716.
- Gardner WL. 1998. Epidermal regulation of dermal fibroblasts activity. *Plast Reconstr Surg* 102:135–139.
- Ghaffari A, Li Y, Karami A, Ghaffari M, Tredget EE, Ghahary A. 2006. Fibroblast extracellular matrix gene expression in response to keratinocyte-releasable stratifin. *J Cell Biochem* 98:383–393.
- Ghaffari A, Kilani RT, Ghahary A. 2009. Keratinocyte-conditioned media regulate collagen expression in dermal fibroblasts. *J Invest Dermatol* 129:340–347.
- Ghahary A, Tredget EE, Shen Q, Kilani RT, Scott PG, Houle Y. 2000. Mannose-6-phosphate/IGF-II receptors mediate the effect of IGF-1-induced latent transforming growth factor beta 1 on expression of type I collagen and collagenase in dermal fibroblasts. *Growth Factors* 17:167–176.
- Ghahary A, Marcoux Y, Karami-Busheri F, Tredget EE. 2001. Keratinocyte differentiation inversely regulates the expression of involucrin and transforming growth factor beta-1. *J Cell Biochem* 83:239–248.
- Ghahary A, Karami-Busheri F, Marcoux Y, Li Y, Tredget EE, Kilani RT, Li L, Zheng J, Karami A, Keller BO, Weinfeld M. 2004. Keratinocyte-releasable stratifin functions as a potent collagenase-stimulating factor in fibroblasts. *J Invest Dermatol* 122:1188–1197.
- Harrison CA, Dalley AJ, Mac Neil S. 2005. A simple in vitro model for investigating epithelial/mesenchymal interactions: Keratinocyte inhibition of fibroblast proliferation and fibronectin synthesis. *Wound Repair Regen* 13:543–550.
- Harrison CA, Gossiel F, Bullock AJ, Sun T, Blumsohn A, Mac Neil S. 2006. Investigation of keratinocyte regulation of collagen I synthesis by dermal fibroblasts in a simple in vitro model. *Br J Dermatol* 154:401–410.
- Hohenester E, Maurer P, Hohenadl C, Timpl R, Jansonius JN, Engel J. 1996. Structure of a novel extracellular Ca(2+)-binding module in BM-40. *Nat Struct Biol* 3:67–73.
- Katz AB, Taichman LB. 1999. A partial catalog of proteins secreted by epidermal keratinocytes in culture. *J Invest Dermatol* 112:818–821.
- Kozakov D, Brenke R, Comeau SR, Vajda S. 2006. PIPER: An FFT-based protein docking program with pairwise potentials. *Proteins* 65:392–406.
- Kozakov D, Hall DR, Beglov D, Brenke R, Comeau SR, Shen Y, Li K, Zheng J, Vakili P, Paschalidis I, Vajda S. 2010. Achieving reliability and high accuracy in automated protein docking: ClusPro, PIPER, SDU, and stability analysis in CAPRI rounds 13–19. *Proteins* 78:3124–3130.
- Ladak A, Tredget EE. 2009. Pathophysiology and management of the burn scar. *Clin Plast Surg* 36:661–674.
- Lane TF, Sage EH. 1994. The biology of SPARC, a protein that modulates cell-matrix interactions. *FASEB J* 8:163–173.
- Machesney M, Tidman N, Waseem A, Kirby L, Leigh I. 1998. Activated keratinocytes in the epidermis of hypertrophic scars. *Am J Pathol* 152:1133–1141.
- Morris D, Wu L, Zhao LL, Bolton L, Roth SI, Ladin DA, Mustoe TA. 1997. Acute and chronic animal models for excessive dermal scarring: Quantitative studies. *Plast Reconstr Surg* 100:674–681.
- Nowinski D, Lysheden AS, Gardner H, Rubin K, Gerdin B, Ivarsson M. 2004. Analysis of gene expression in fibroblast in response to keratinocyte-derived factors in vitro: Potential implications for the wound healing process. *J Invest Dermatol* 122:216–221.
- Ralston DR, Layton C, Dalley AJ, Boyce SG, Freedlander E, Mac Neil S. 1997. Keratinocytes contract human dermal extracellular matrix and reduce soluble fibronectin production by fibroblasts in a skin composite model. *Br J Plast Surg* 50:408–415.
- Reed MJ, Sage EH. 1996. SPARC and the extracellular matrix: Implications for cancer and wound repair. *Curr Top Microbiol Immunol* 213:81–94.
- Rentz TJ, Poobalarahi F, Bornstein P, Sage EH, Bradshaw AD. 2007. SPARC regulates processing of procollagen 1 and collagen fibrillogenesis in dermal fibroblasts. *J Biol Chem* 282:22062–22071.
- Wilker EW, Grant RA, Artim SC, Yaffe MB. 2005. A structural basis for 14-3-3 sigma functional specificity. *J Biol Chem* 280:18891–18898.
- Wood FM, Stoner M. 1996. Implication of basement membrane development on the underlying scar in partial-thickness burn injury. *Burns* 22:459–462.